Tuning the in-plane electron behavior in high-T_c cuprate superconductors via apical atoms: A first-principles Wannier-states analysis

Wei-Guo Yin[1,*] and Wei Ku[1,2,†]

[1]*Department of Condensed Matter Physics and Materials Science, Brookhaven National Laboratory, Upton, New York 11973, USA*

[2]*Department of Physics, State University of New York, Stony Brook, New York 11790, USA*

(Received 7 April 2009; published 12 June 2009)

Using a recently developed first-principles Wannier-states approach that takes into account large on-site Coulomb repulsion, we derive the low-energy effective one-band Hamiltonians for several prototypical cuprate superconductors. The material dependence is found to originate primarily from the different energy of the apical atom p_z state. Specifically, the general properties of the low-energy hole state, namely, the Zhang-Rice singlet, are significantly modified, via additional intrasublattice hoppings, nearest-neighbor "super repulsion," and other microscopic many-body processes. Implications on modulations of local pairing gaps, charge distribution, hole-hopping range, electron-phonon interaction, and multilayer effects in cuprate superconductors are discussed.

DOI: 10.1103/PhysRevB.79.214512 PACS number(s): 74.72.−h, 71.10.−w, 74.25.Jb, 74.40.+k

I. INTRODUCTION

The origin of high-T_c superconductivity (HTSC) remains under fierce debate notwithstanding monumental effort for two decades. Although it is generally agreed that the most relevant electron behavior is confined within the common CuO_2 plane,[1–8] $T_c^{\max}$ (T_c at optimal doping) is strikingly affected by modulation of the layering pattern along the less essential third direction.[9–12] Hence, clarifying the *material dependence* of the in-plane electron behavior, especially with material-specific first-principles approaches, is an essential step toward the resolution of the HTSC mechanism and the quest for higher-T_c superconductors.

A recent influential advancement along the line was made by Pavarini *et al.*:[12] within the local-density approximation (LDA) of density-functional theory (DFT) for a number of hole-doped cuprates, they derived a one-band *noninteracting* Hamiltonian in which $|t'/t|$ (t and t' are the in-plane first- and second-nearest-neighbor hopping integrals, respectively) appeared to correlate with $T_c^{\max}$ and was related to out-of-plane (apical) atoms. Taken as the kinetic part of the effective one-band t-J or Hubbard model, the most studied model for the CuO_2 plane,[1–7] this single band has been widely used to compare with angular-resolved photoemission spectroscopy (ARPES).[8,13,14]

A particular puzzle thus caused is that the LDA $|t'/t|=0.18$ for La_2CuO_4 and 0.12 for $Ca_2CuO_2Cl_2$ (Ref. 12) contradict with their diamondlike and squarelike Fermi surfaces, respectively, as observed in ARPES.[8,13,15] In addition, the suggested t' effect on T_c (Refs. 10–12) turned out to be controversial in several numerical studies of the extended t-J or Hubbard model.[16–18] More importantly, all LDA derived one-band metallic picture suffers from a fundamental deficiency of single-particle pictures, namely, the doped hole residing in Cu d orbital that hybridizes with O p. This drastically contradicts with the well-established experimental fact that doped holes reside primarily in the oxygen atoms.[19–21] In fact, it is now commonly accepted that the doped holes form spin-singlet states with the intrinsic holes in Cu, the so-called Zhang-Rice singlet (ZRS), in the underdoped region—it is based on ZRS that the one-band t-J or Hubbard model has been justified.[1–7] Thus, it is important to examine the material dependence of general electron behavior in the CuO_2 plane by deriving an effective *interacting* Hamiltonian with a first-principles approach that takes into account, from the beginning, large Coulomb repulsion on the Cu sites. Such studies would not only produce a more appropriate character of low-energy states but also reveal new material-dependent physical effects derived from the charge-transfer nature and the complexity of strong electronic correlation.

In this paper, we address this issue by extending the recently developed first-principles Wannier-states (WSs) approach[22,23] to low-energy scale (~ 1 eV). The material dependence is found to originate primarily from different ε_{p_z}, the energy of the apical atom p_z state, in accord with the fact that the apical coordination of Cu ions is the main structural variation relevant to the CuO_2 plane.[24] In the present work, the entire range of ε_{p_z} (approaching the Fermi level E_F from infinity) is represented by four prototypical cuprates: Nd_2CuO_4, $Sr_2CuO_2F_2$, $Ca_2CuO_2Cl_2$, and La_2CuO_4, where the apical sites are empty, F, Cl, and O, respectively. The proximity of ε_{p_z} to E_F is found to suppress $|t'/t|$ *of* ZRS, resolving the aforementioned puzzle in existing first-principles results on $Ca_2CuO_2Cl_2$. More interestingly, this proximity generates several crucial many-body effects, including local site-dependent potentials and a remarkable intersite "super-repulsion," which directly modulate local pairing gaps and charge distribution, and imply an intriguing realization of electron-phonon coupling. These findings would shed light on the general material dependence and microscopic understanding of HTSC.

II. METHODS

A three-step approach is used to reduce systematically the energy scale of the relevant Hilbert space:

A. At full-energy scale

The full-energy electronic structures of the undoped system are obtained within the LDA+U method (with U

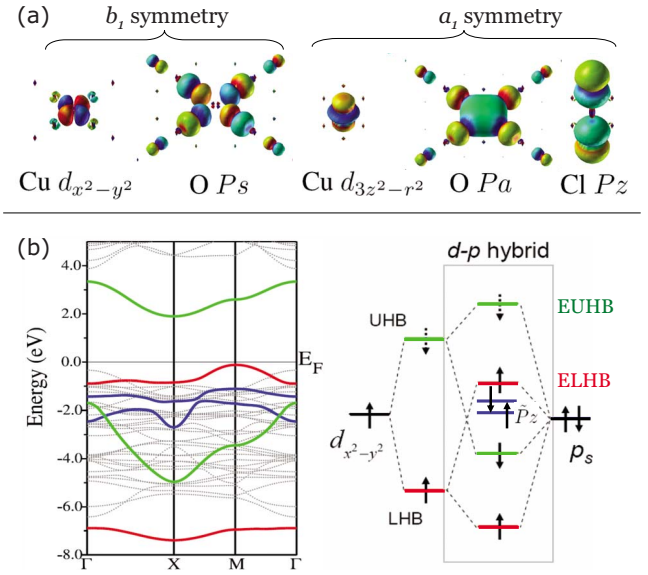

FIG. 1. (Color online) (a) Wannier functions centered at Cu sites for H^{5b}: O P_s and P_a are constructed by maximizing the weight of the b_1- and a_1-symmetrized combinations of four neighboring planar O p_σ orbitals, respectively, P_z is the a_1-symmetrized combination of two apical p_z orbitals. (b) Left panel: band structure of $Ca_2CuO_2Cl_2$ from LDA+U calculations (dots) and the bands mainly of $Cu_{x^2-y^2}$, O P_s, and apical P_z characters from Wannier-states analysis (lines). $\Gamma=(0,0,0)$, $X=(\pi,0,0)$, and $M=(\frac{\pi}{2},\frac{\pi}{2},0)$. Right panel: corresponding local energy-level splitting due to interactions and d-p hybridization filled with electrons (solid arrows) or holes (dashed arrows). Up and down arrows denote spin majority and spin minority, respectively. $\tilde{P}z$ derived from two highest a_1 hybrids are mainly of apical P_z character. EUHB (ELHB) means the effective upper (lower) Hubbard subband.

$=8$ eV and $J=0.88$ eV) (Ref. 25) known as a state-of-the-art generalization of LDA to include strong local interaction. This provides a good first-principles *starting point* since it correctly predicts a charge-transfer insulator as the ground state instead of a metallic state from LDA, as shown in the left panel of Fig. 1(b) for $Ca_2CuO_2Cl_2$ as an example. In addition, the choice of *insulating* undoped system avoids the serious deficiency of current approximations of density-functional theory in treating the strong quantum fluctuation (which is suppressed by the existence of the gap). We have applied the WIEN2K (Ref. 26) implementation of the full-potential linearized augmented-plane-wave method in the LDA+U approach and verified that our conclusions are unaffected for $U=6.5-10$ eV.

B. At the intermediate-energy scale (~10 eV)

At the intermediate-energy scale (~10 eV covering relevant Cu 3d, O 2p, and apical orbitals), an effective Hubbard-type five-band interacting Hamiltonian, H^{5b}, is derived via the WSs analysis of the LDA+U results.[22]

The five most relevant WSs whose characters appear in low-energy bands near E_F are *defined* in Fig. 1(a). We note that all the oxygen Wannier functions are constructed to center at the copper sites; P_s, P_a, and P_z are obtained by maximizing the weights of the following symmetrical combination of the "atomic" oxygen 2p σ orbitals, respectively,

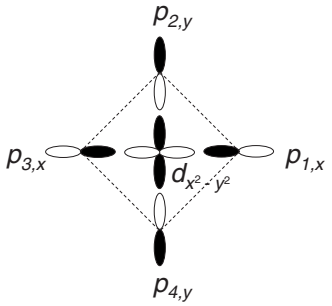

FIG. 2. The planar atomic orbitals in a CuO_4 plaquette. The shown b_1-symmetrized pattern is for O P_s.

$$P_s: \frac{1}{2}(p_{1,x}+p_{2,y}+p_{3,x}+p_{4,x}),$$

$$P_a: \frac{1}{2}(p_{1,x}-p_{2,y}+p_{3,x}-p_{4,x}),$$

$$P_z: \frac{1}{\sqrt{2}}(p_{5,z}+p_{6,z}),$$

where $p_{5,z}$ and $p_{6,z}$ are the apical (out-of-plane) oxygen 2p_z orbitals and the rest (planar) are illustrated in Fig. 2, compared with Fig. 1(a). In this representation, the decorated CuO_2 plane reduces to a regular simple square lattice where each lattice site represents a "super Cu atom" which includes the three oxygen Wannier orbitals. This avoids the difficulty in defining the local subsystem due to having a bridging site between two Cu sites. Now that both electron-electron interaction and leading d-p hybridization become *local* terms, it is convenient to treat their effects exactly on the local multiplets and the remaining nonlocal parts as perturbation.

In the left panel of Fig. 1(b), we present the bands mainly of Cu $d_{x^2-y^2}$, O P_s, and apical P_z characters, the three most relevant Wannier orbitals (instead of all the five orbitals in an effort to make the plot less crowded), in accord with the x-ray absorption spectra.[27] The strong *local* d-d interactions and d-p hybridizations between the b_1-symmetrized Cu $d_{x^2-y^2}$ and O P_s Wannier orbitals are illustrated in the right panel. In this illustration, the leftmost and rightmost orbitals (before spin polarization and d-p hybridization) correspond to the Cu $d_{x^2-y^2}$ and O P_s basis Wannier functions plotted in Fig. 1(a), respectively. The on-site hopping parameter between them is 2.35 eV. Clearly, the Hubbard splitting of the Cu $d_{x^2-y^2}$ spin-majority and spin-minority WSs severely affects hybridization between Cu $d_{x^2-y^2}$ and O P_s. Consequently, the lowest-unoccupied and highest-occupied bands (though both derived from antibonding between $d_{x^2-y^2}$ and P_s) are mainly of spin-minority $d_{x^2-y^2}$ and spin-majority P_s characters, respectively, in agreement with the experimentally observed low-energy quasiparticle characters: doped holes residing primarily on the oxygen atoms[19,20] and forming the spin-singlet states with the intrinsic holes on the Cu atoms. Therefore, the lowest unoccupied and highest-

TABLE I. Selected parameters in Eq. (1) obtained from the Wannier-states analysis of the LDA+U ground-state electron structures of $Ca_2CuO_2Cl_2$. D_x stands for $d_{x^2-y^2}$ and D_z for $d_{3z^2-r^2}$. nn denotes nearest neighbor. The unit is eV.

	On-site		1st nn	2nd nn	3rd nn
U_{eff}	9.625	T_{ij}^{PsDx}	0.388	0.034	0.092
U'_{eff}	6.754	T_{ij}^{PsPs}	0.288	0.185	0.076
J_{eff}	0.706	T_{ij}^{DxDx}	0.032	0.003	0.002
ϵ_d	0.964				
ϵ_{Ps}	2.003	T_{ij}^{PsPz}	0.129		0.029
ϵ_{Pa}	4.111	T_{ij}^{PsDz}	0.130		0.030
ϵ_{Pz}	2.812	T_{ij}^{PsPa}	0.065		0.003
T_{ij}^{PsDx}	2.351	T_{ij}^{DxPz}	0.026		0.006
T_{ij}^{DzPa}	0.845	T_{ij}^{DxDz}	0.034		0.003
T_{ij}^{PzPa}	0.778	T_{ij}^{DxPa}	0.354		0.084
T_{ij}^{PzDz}	0.951				

occupied bands may be loosely regarded as the effective upper and lower Hubbard subbands, respectively, with the d-p charge-transfer gap as the effective Hubbard gap. In addition, note that their overall shapes—the top of the valence band is at $(\pi/2,\pi/2)$ and the bottom of the conduction band at $(\pi,0)$, agree well with ARPES,[8] further confirming that the LDA+U calculation is indeed a good starting point. On the other hand, their bandwidths are doubly overestimated due to neglecting strong electronic correlation at this step, to be remedied at the next step.

There are considerable nearest-neighbor hoppings between b_1 ($d_{x^2-y^2}$, P_s) and a_1 ($d_{3z^2-r^2}$, P_a, and P_z) orbitals but by symmetry these five WSs almost completely decouple from other WSs. Hence, they form a practically complete basis for the low-energy Hilbert space. Within this five-orbital basis set, H^{5b}, including all possible one-particle terms and on-site intraorbital and interorbital Coulomb repulsions and exchange interaction in the Cu d WSs (referred to as U_{eff}, U'_{eff}, and J_{eff}, respectively),[11] is given by

$$H^{5b} = \sum_{ijmm'\sigma} (T_{ij}^{mm'} C_{im\sigma}^{\dagger} C_{jm'\sigma} + \text{H.c.}) + \sum_{im\sigma} \varepsilon_m n_{im\sigma} + U_{\text{eff}} \sum_{i,m=1,2} n_{im\uparrow} n_{im\downarrow} + U'_{\text{eff}} \sum_{i\sigma\sigma'} n_{i1\sigma} n_{i2\sigma'} - J_{\text{eff}} \sum_{i\sigma\sigma'} C_{i1\sigma}^{\dagger} C_{i1\sigma'} C_{i2\sigma'}^{\dagger} C_{i2\sigma}, \quad (1)$$

where $C_{im\sigma}$ annihilates an electron with spin σ in the mth Wannier state at site i. Here $m=1,2,\ldots,5$ stand for Cu $d_{x^2-y^2}$, Cu $d_{3z^2-r^2}$, planar O P_s, planar O P_a, and apical O P_z Wannier orbitals, respectively.

All the parameters in H^{5b} can be *calculated out* by using the following scheme: since LDA+U treats the interaction in the localized orbitals in an effective Hartree-Fock (HF) approach, a clear mapping can be achieved by matching the corresponding Wannier representation of the LDA+U one-particle Hamiltonian, $H_{im\sigma,jm'\sigma}^{\text{LDA}+U}$, to the self-consistent HF expression of H^{5b}. This scheme is well controlled and has been shown to work well for manganites.[22] More specifically,

(1) $T_{ij}^{mm'}$, all the hopping integrals, are directly given by $T_{ij}^{mm'} = H_{im\sigma,jm'\sigma}^{\text{LDA}+U}$.

(2) ε_{im} for $m=3,4,5$, the site energy of the oxygen Wannier states, are given by $\varepsilon_{im} = H_{im\sigma,im\sigma}^{\text{LDA}+U}$.

(3) The remaining four parameters ε_d (assume $\varepsilon_d = \varepsilon_{i1} = \varepsilon_{i2}$), U_{eff}, U'_{eff}, and J_{eff} are determined by the four matrix elements $H_{im\sigma,im\sigma}^{\text{LDA}+U}$ for $m=1,2$ and $\sigma=\uparrow,\downarrow$ in self-consistent Hartree-Fock theory where the diagonal mean fields $\langle n_{im\sigma}\rangle$ already known from the LDA+U density matrix, which also reveals that other mean fields are negligible. Therefore, it turns out to simply solve the following system of four linear equations,

$$H_{i1\uparrow,i1\uparrow}^{\text{LDA}+U} = \varepsilon_d + U_{\text{eff}}\langle n_{i1\downarrow}\rangle + U'_{\text{eff}}\langle n_{i2}\rangle - J_{\text{eff}}\langle n_{i2\uparrow}\rangle,$$

$$H_{i1\downarrow,i1\downarrow}^{\text{LDA}+U} = \varepsilon_d + U_{\text{eff}}\langle n_{i1\uparrow}\rangle + U'_{\text{eff}}\langle n_{i2}\rangle - J_{\text{eff}}\langle n_{i2\downarrow}\rangle,$$

$$H_{i2\uparrow,i2\uparrow}^{\text{LDA}+U} = \varepsilon_d + U_{\text{eff}}\langle n_{i2\downarrow}\rangle + U'_{\text{eff}}\langle n_{i1}\rangle - J_{\text{eff}}\langle n_{i1\uparrow}\rangle,$$

$$H_{i2\downarrow,i2\downarrow}^{\text{LDA}+U} = \varepsilon_d + U_{\text{eff}}\langle n_{i2\uparrow}\rangle + U'_{\text{eff}}\langle n_{i1}\rangle - J_{\text{eff}}\langle n_{i1\downarrow}\rangle,$$

where $n_{im} = \Sigma_\sigma n_{im\sigma}$.

Note that this scheme works for a more general Hamiltonian. At first glance, the unknown parameters of a general Hamiltonian seems to be more than the known matrix elements of $H^{\text{LDA}+U}$, rendering the problem to be underdetermined. Actually, more known matrix elements can be generated by additional LDA+U calculations for different structures and/or orbital/spin configurations, which eventually renders the problem to be overdetermined and thus become a fitting task.[22]

The results for $Ca_2CuO_2Cl_2$—except for the less important $T_{ij}^{mm'}$ among the a_1 orbitals ($d_{3z^2-r^2}$, P_a, and P_z)—are presented in Table I. Here the averaged effective Coulomb interaction on the d orbitals is $U_{\text{eff}}^{\text{ave}} = 0.2U_{\text{eff}} + 0.8U'_{\text{eff}} = 7.4$ eV and $J_{\text{eff}} = 0.7$ eV. These values are close to the LDA+U inputs for d *atomic* orbitals [$U=8.0$ eV and $J=0.88$ eV (Ref. 25)], indicating that the Cu d *Wannier* orbit-

als determined at the 10 eV energy scale are well localized. In addition, note that nearest-neighbor $T_{ij}^{D_xP_s}=0.39$ eV and $T_{ij}^{D_xP_a}=0.35$ eV are similar, substantially different from $T_{ij}^{D_xP_s}=0.36$ eV and $T_{ij}^{D_xP_a}=0$ eV derived in the formalism used in previous studies.[4–7,11] The present numbers confirm that overall the Wannier functions constructed in our approach are more localized. On the other hand, we have tested that these two different gauges of the Wannier functions lead to the same conclusions.

In comparison, the conventional approach to the one-particle parameters (i.e., fitting the hopping parameters to the band structure) is not well controlled. For example, the direct in-plane O-O hopping t_{pp} between $p_{1,x}$ and $p_{2,y}$ in Fig. 1, which controls the value of t' in the final one-band Hamiltonian, was reported to vary from 0.04 to 0.65 eV.[28] Large t_{pp} means that the O p orbitals are quite extended and thus the effects of Coulomb interaction in the oxygen orbitals may be insignificant. Here by constructing the atomic $p_{1,x}$ and $p_{2,y}$ Wannier functions we confirm that $t_{pp}\simeq 0.65$ eV.

Note that to study the spontaneous symmetry breaking in the system, it is convenient to construct Hamiltonian (1) based on spin-independent Wannier orbitals. However, recall that our Wannier functions are constructed within a finite-energy window (i.e., the limited number of bands) for the intermediate- or low-energy physics. This means that they are in principle spin dependent within the spin-polarized DFT calculations because the spin independency cannot be fully recovered when the orbitals outside the energy window are spin polarized, more or less, via electron-electron interaction or hybridization. This results in the spin-dependent hopping parameters. On the other hand, *the degree of this spin dependency provides a practical way to judge whether the chosen energy window is sufficiently large*. It was attempting to directly build a one-band model using only the lowest-unoccupied and highest-occupied bands for, as mentioned above, they may be loosely regarded as the effective upper and lower Hubbard subbands, respectively; the resulting hopping parameters turned out to be strongly spin dependent. The hopping parameters in the five-orbital Hamiltonian (1), are obtained from averaging those in the spin-majority channels and their counterparts in the spin-minority channel. The deviation from the average is less than 7% for all the leading hopping parameters (whose magnitude is larger than 0.06 eV). Therefore, we conclude that it is appropriate to approximate the ten slightly spin-polarized Wannier functions with the above spin-independent treatment.

C. At the low-energy scale (~1 eV)

At the low-energy scale (~1 eV), an effective one-band Hamiltonian, H^{1b}, for the doped holes is derived from canonical transformation (CT) of H^{5b} to the second order.[4–7,11,29]

To reduce the multiband Hubbard model to a one-band model, we follow Hubbard's atomic representation approach,[29–33] in which H is rewritten in terms of the multiplets of its one-unit cell part solved by exact diagonalization. Here the local part of H^{5b}, which includes the leading terms (on-Cu-site interactions and local d-p hybridizations), is diagonalized for all doping levels.[11,29] In particular, our approach benefits greatly from having all the *first-principles* WSs, including the O $2p$ states, centered at the Cu sites by construction [see Fig. 1(a)]. This reduces the decorated CuO_2 lattice to a simple square lattice and unambiguously defines the local Hamiltonian to be diagonalized.[4–7,11] For $Ca_2CuO_2Cl_2$, the local one-hole ground state (referred to as $|\sigma\rangle$) with energy $E_1=-2.26$ eV is a hybrid of $d_{x^2-y^2}$ (76%) and P_s (24%), and the first-excited one-hole state with energy −1.38 eV is a hybrid of $d_{3z^2-r^2}$ (91%), P_a (6%), and P_z (3%); thus, the local $d_{x^2-y^2}\rightarrow d_{3z^2-r^2}$ excitation energy (Δ_1) is 0.88 eV. The local two-hole ground state is the ZRS of two b_1 holes (referred to as $|\mathrm{ZRS}\rangle$) with energy $E_2=-1.96$ eV, and the first-excited two-hole state is a spin triplet (referred to as $|\mathrm{axial}\rangle$) of one b_1 hole and the other in the a_1 states; the $|\mathrm{ZRS}\rangle\rightarrow|\mathrm{axial}\rangle$ excitation energy (Δ_2) is 0.81 eV. In addition, the spin-triplet state of two b_1 holes (the Emery-Reiter triplet) is 3.3 eV higher than the ZRS. Therefore, it may be appropriate to keep in the low-energy space only $|\sigma\rangle$, $|\mathrm{ZRS}\rangle$ and integrate out all the other states by canonical transformation[29] or perturbation to the second order.[33]

Suppose $H=H_0+H_1$ and define $H(\lambda)=H_0+\lambda H_1$. Then, the transformed Hamiltonian is

$$H_S(\lambda)=e^{-\lambda S}He^{\lambda S}\simeq H_0+\frac{\lambda^2}{2!}[H_1,S], \tag{2}$$

after removing the terms linear with respect to λ following

$$\lambda H_1+[H_0,\lambda S]=0. \tag{3}$$

Let us apply the above canonical transformation to Eq. (1). First define the Hubbard operator on the ith site as

$$X_i^{pq}=|p\rangle_i\langle q|_i, \tag{4}$$

and the projection operator as

$$P_0=\prod_i \sum_{p\in \mathrm{g.s.}} X_i^{pp}, \quad P_1=1-P_0, \tag{5}$$

where g.s. means the ground-state multiplets (the states we want to keep); here they are $|\sigma\rangle$ and $|\mathrm{ZRS}\rangle$. Then, H_0 and H_1 may be defined by

$$\begin{aligned} H_0=P_0HP_0+P_1HP_1=&\sum_i\sum_p \epsilon_{ip}X_i^{pp} \\ &+P_0\sum_{i<j}\sum_{rr's's'}(V_{ij}^{rr',ss'}X_i^{rr'}X_j^{ss'}+\mathrm{H.c.})P_0 \\ &+P_1\sum_{i<j}\sum_{rr's's'}(V_{ij}^{rr',ss'}X_i^{rr'}X_j^{ss'}+\mathrm{H.c.})P_1, \end{aligned} \tag{6}$$

and

$$\begin{aligned} H_1=P_0HP_1+P_1HP_0=&P_0\sum_{i<j}\sum_{rr's's'}(V_{ij}^{rr',ss'}X_i^{rr'}X_j^{ss'}+\mathrm{H.c.})P_1 \\ &+P_1\sum_{i<j}\sum_{rr's's'}(V_{ij}^{rr',ss'}X_i^{rr'}X_j^{ss'}+\mathrm{H.c.})P_0. \end{aligned} \tag{7}$$

From Eq. (3) on the condition we neglect the intersite terms,

TABLE II. ε_{Pz} and parameters of Eq. (10) for four prototypical cuprates upon hole doping. Inside parentheses are contributions purely from the b_1 orbitals. The energy unit is meV.

	Nd_2CuO_4	$Sr_2CuO_2F_2$	$Ca_2CuO_2Cl_2$	La_2CuO_4
$\varepsilon_{Pz}-\varepsilon_{Ps}$ [a]	∞	3010	810	280
$J_{\mathrm{LDA}+U}$ [b]	131	155	145	144
$J/2$	138 (138)	138 (138)	131 (131)	129 (129)
t	431 (431)	467 (467)	459 (459)	488 (488)
$t'/\lvert t\rvert$	−0.33 (−0.35)	−0.25 (−0.32)	−0.19 (−0.32)	0.01 (−0.30)
$t''/\lvert t\rvert$	0.23 (0.24)	0.19 (0.23)	0.16 (0.23)	0.06 (0.22)
V_{ij}	29 (27)	39 (29)	54 (30)	137 (31)
μ_i	−795 (−800)	−337 (−394)	−295 (−412)	−354 (−529)
ε_{ij}	−36 (−14)	−86 (−17)	−133 (−17)	−258 (−19)

[a] ε_{Ps} denotes the site energy of the O P_s state.
[b] Estimated from total-energy difference between the ferromagnetic and antiferromagnetic states.

$$S \simeq P_0 \sum_{i<j} \sum_{rr's's'} (A_{ij}^{rr',ss'} X_i^{rr'} X_j^{ss'} - \mathrm{H.c.}) P_1 + P_1 \sum_{i<j} \sum_{rr's's'} (A_{ij}^{rr',ss'} X_i^{rr'} X_j^{ss'} - \mathrm{H.c.}) P_0, \quad (8)$$

where

$$A_{ij}^{rr',ss'} = \frac{V_{ij}^{rr',ss'}}{\epsilon_{r'} + \epsilon_{s'} - \epsilon_r - \epsilon_s}. \quad (9)$$

This gives rise to the one-band t-J-type Hamiltonian, or t-U Hamiltonian with effective $U \simeq E_2 - 2E_1 = 2.56$ eV when the no-hole vacuum state is also retained. Here the t's stand for the intersite exchange of the $|\mathrm{ZRS}\rangle$ and $|\sigma\rangle$ states.[4–7]

$$H^{1b} = -\sum_{ij\sigma} t_{ij} (\tilde{c}_{i\sigma}^{\dagger} \tilde{c}_{j\sigma} + \mathrm{H.c.}) + J \sum_{\langle ij \rangle} \left(\vec{S}_i \cdot \vec{S}_j - \frac{n_i n_j}{4} \right) + \frac{J}{4} \sum_{\langle ijk \rangle \sigma} (\tilde{c}_{i\sigma}^{\dagger} \tilde{c}_{j\bar{\sigma}}^{\dagger} \tilde{c}_{j\sigma} \tilde{c}_{k\bar{\sigma}} - \tilde{c}_{i\sigma}^{\dagger} n_{j\bar{\sigma}} \tilde{c}_{k\sigma} + \mathrm{H.c.}) + \sum_{\langle ij \rangle} V_{ij} n_i n_j + \sum_i \mu_i n_i + \sum_{\langle ij \rangle} \varepsilon_{ij}, \quad (10)$$

where the notation follows the standard t-J model[1–7] and t_{ij} extends to the third nearest neighbors (t''). Tiny corrections of three-site hopping terms including $\tilde{c}_{i\sigma}^{\dagger}(1-n_j)\tilde{c}_{k\sigma}$ have been neglected. The first two lines of Eq. (10) resemble the t-J model mapped from the one-band Hubbard model and have been extensively studied.[1–3] The other terms include *locally* ε_{Pz}-dependent super-repulsion V_{ij}, site potential μ_i, and energy "constant" ε_{ij} (only relevant to equilibrating apical atoms).

Note that we have implemented all the Hamiltonians, the Hubbard operators, and the commutators as the C++ objects; therefore, Eqs. (1)–(10) were coded literally. This greatly facilitates the otherwise very complicated multiorbital canonical transformation.

III. RESULTS AND DISCUSSION

The material dependence of the cuprates is first quantified via H^{5b} and is found to originate primarily from ε_{Pz}, as shown in Table II. We then present the derived parameters of H^{1b} for the four prototypical cuprates covering the realistic spectrum of ε_{Pz}. For comparison, the contributions purely from the b_1 orbitals (from which ZRS is formed) are given inside the parentheses. Remarkably, *there exists practically no material dependence if only the* b_1 orbitals are considered. The universality for t and J even survives inclusion of the a_1 orbitals since they are solely determined by the b_1 orbitals suggesting the robustness of superconductivity among cuprates. Further, the insignificant contributions of the a_1 orbitals for Nd_2CuO_4, which does *not* have apical atoms, manifest that the demonstrated strong material dependence *almost entirely results from the influence of the apical* P_z orbitals, indeed.

Now we discuss in passing the strong ε_{Pz} dependence of t', t'', V_{ij}, μ_i, and ε_{ij} [cf. Fig. 3(a)]. First of all, three-site kinematical processes via virtual nearest-neighbor hoppings to the P_z orbital dramatically reduce $|t'|$ and $|t''|$, as suggested in Ref. 11. This would seriously affect hole-hopping range and reshape the Fermi surface, given the nearest-neighbor hoppings being suppressed by the antiferromagnetic spin correlation.[1–3] Note that $|t'/t|$ is now substantially smaller in La_2CuO_4 than in $Ca_2CuO_2Cl_2$, in agreement with their observed diamondlike and squarelike Fermi surfaces, respectively.[8,13,15]

The justification of our resulting Hamiltonian can be made by comparing the (approximate) solution with known

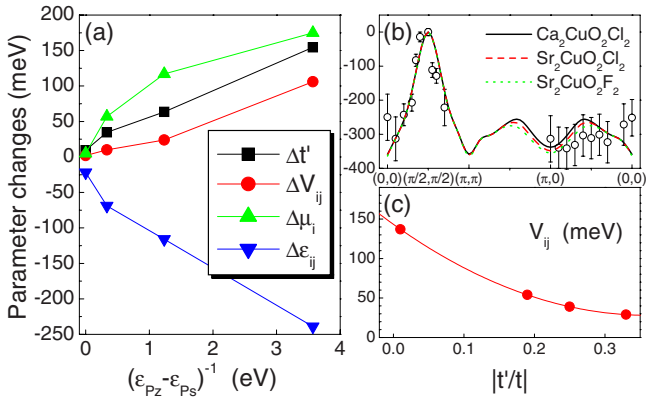

FIG. 3. (Color online) (a) Parameter changes by the a_1 orbitals as a function of ε_{Pz}. (b) Calculated one-hole quasiparticle dispersions compared with ARPES on $Sr_2CuO_2Cl_2$ (open circles) (Ref. 8). (c) V_{ij} versus $|t'/t|$.

experimental data. For the cuprates, much attention has been paid to the ARPES on undoped $A_2CuO_2Cl_2$ (A=Ca,Sr), since they correspond to the single-doped hole case, for which we have so far the cleanest theory in the context of a doped Mott insulator. Compared with the generally known results extrapolated from ARPES on $A_2CuO_2Cl_2$,[34–36] t''/t agrees well but t'/t is smaller by half. Thus, we are motivated to reexamine the single-hole dynamics within the self-consistent Born approximation (SCBA) of the spin-polaron picture,[14,37] whose accuracy for the single-hole problem has been verified by small cluster exact diagonalization.[38] We find that the one-hole quasiparticle dispersions calculated with the present values for $A_2CuO_2X_2$ (A=Ca,Sr; X=F,Cl) in SCBA actually agree well with ARPES,[8] as shown in Fig. 3(b). This is because the hole quasiparticle dispersion is in fact *insensitive* to t', given t''/t=0.2 (Ref. 39), as shown in Fig. 4.

Besides, it is known that the three-site hopping terms can improve the agreement with ARPES.[40,41] It is worth mentioning that the main role of the three-site hopping terms is to suppress t' by $J/2$ and enhance t'' by $J/4$; therefore, the fitted

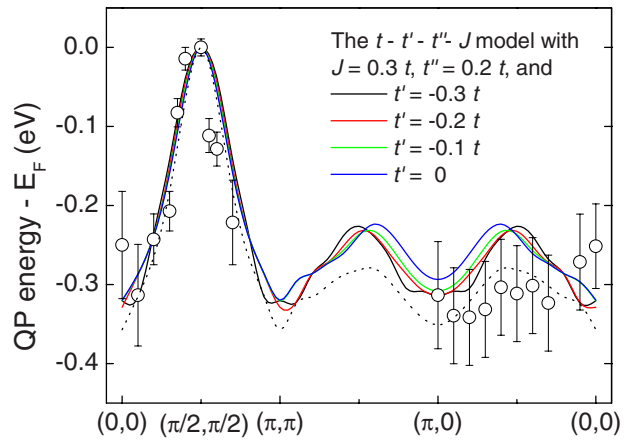

FIG. 4. (Color online) Single-hole quasiparticle dispersion in the SCBA for the t-t'-t''-J models with t=0.5 eV (solid lines), compared with the ARPES results for $Sr_2CuO_2Cl_2$ (Ref. 35) (circles) and the SCBA result for Eq. (2) (dotted line).

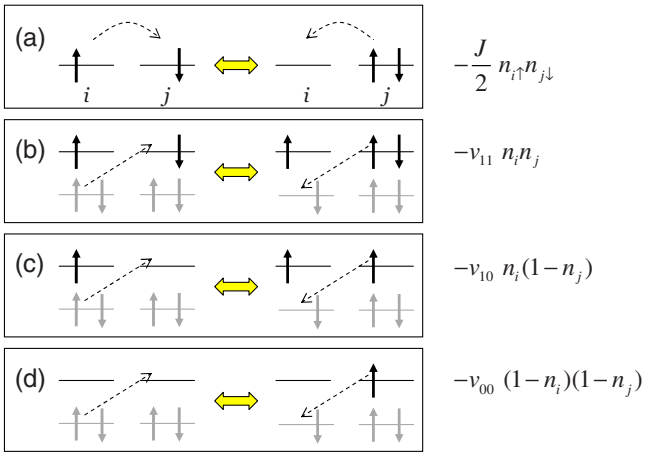

FIG. 5. (Color online) Schematics of virtual kinematical processes (dashed lines) and corresponding effective one-band interactions for (a) Heisenberg superexchange within a one-orbital system and (b)–(d) additional "vacuum fluctuations" in a two-orbital system. Electrons (solid arrows) in the targeted and projected out orbitals are black and gray, respectively.

values of t' and t'' depend sensitively on inclusion of the three-site hopping terms.[39] Our first-principles derived Hamiltonian finally provides an unambiguous benchmark of these material-dependent parameters.

In contrast, while the role of apical atom in determining the t'/t ratio was also emphasized in the LDA "downfolding" procedure, the LDA one band led to a puzzling trend ($|t'/t|$=0.18 for La_2CuO_4 and 0.12 for $Ca_2CuO_2Cl_2$) (Ref. 12) that appears opposite to ARPES and ours. This is, however, not alarming due to intrinsic differences in the meaning of t's: t's in H^{1b} actually describe intersite swapping of two-hole $|\mathrm{ZRS}\rangle$ and one-hole $|\sigma\rangle$ states,[4–7] whereas LDA t's describe hoppings between single-particle LDA $|\sigma\rangle$ states.[12] Clearly, building strong many-body characteristics in first-principles approaches *before* the downfolding,[4–7] as presented here, is necessary for the low-energy physics of cuprates.

Next, we elaborate the kinematic origin of the super-repulsion V_{ij} in our derivation, and its significant implications due to its strong material (p_z) dependence. For a purely one-band system in the large on-site repulsion limit [Fig. 5(a)], the virtual hoppings between two singly occupied neighboring sites generate the well-known superexchange effect $-\frac{J}{2}n_{i\sigma}n_{j\bar{\sigma}}$. Given an extra fully occupied orbital to be projected out (P_z in the present work), additional virtual kinematical processes give rise to three additional spin-independent terms [$\propto v_{00}$, v_{10}, and v_{11}; see Figs. 5(b)–5(d)] to the targeted one-band Hamiltonian, leading to $V_{ij}=2v_{10}-v_{00}-v_{11}$, $\mu_i=4(v_{00}-v_{10})$, and $\varepsilon_{ij}=-v_{00}$.

Clearly, this effective nearest-neighbor (nn) repulsion, named super-repulsion in analog to superexchange, *is to be distinguished from the nn Coulomb interaction*, although they share the same form. It is believed by many[1–3] that the superconducting pairing scale is controlled by the effective attraction via the nn superexchange J *less* the screened nn Coulomb repulsion (assuming that the electronic screening is efficient and the Coulomb repulsion beyond nn could be

neglected).[42] In the most intensively studied type of the *t-J* models,[1–3] the nn repulsion has not been explicitly included and J should be understood as an effective one that has absorbed the effect of the nn repulsion. However, since J and the nn repulsion are in the spin and charge channels, respectively, it is unclear whether the effect of the nn repulsion could be satisfactorily absorbed into an effective J. It was also argued that compared with J, the nn Coulomb repulsion is screened so much that its appreciable effect is to prevent the phase separation of charge-poor vs charge-rich regions.[43,44] Anyway, the material dependence of the nn repulsion has not been seriously considered. We emphasize that the super-repulsion, V_{ij}, revealed here comes from the virtual processes involving the apical oxygen P_z states. Therefore, it is not only little affected by the normal electron screening of the electrostatic Coulomb interaction but also sensitive to the actual energy of the apical oxygen P_z states. We have shown that the super repulsion can be tuned to be of the same order of magnitude as J by changing the relative energy level of the apical oxygen P_z states. Hence, V_{ij} has crucial effects on the material dependence of the low-energy physics in the cuprates, which is the subject of this work.

V_{ij} apparently weakens local pairing strength, *regardless* of the actual pairing mechanism, given that paired electrons tend to reside as neighbors—implied by the *d*-wave symmetry of the superconducting order parameter in the cuprates.[45] This suggests a fresh look at the material dependence of $T_c^{\max}$. Unlike in the conventional superconductors where electron pairing and the building of the phase coherence among the electron pairs take place at the same time, electron pairing in the underdoped cuprates is likely to occur at a higher temperature than T_c with the pairing scale being reflected as a pseudogap in the spin-excitation spectrum.[1,8,46,47] In this scenario, T_c actually measures the phase coherency of the preformed pairs and is thus more sensitive to disorder and other "extrinsic" properties of real materials than the pseudogap size. Hence, *the material dependence of the pseudogap size (i.e., the pairing scale) would be a more robust link to the material dependence of the intrinsic electronic structure*. For instance, the pseudogap sizes in $Ca_{2-x}Na_xCuO_2Cl_2$ ($T_c^{\max}=28$ K) and $La_{2-x}Sr_xCuO_4$ ($T_c^{\max}=38$ K) (Refs. 8 and 13) do reasonably agree with the V_{ij} trend (the larger V_{ij}, the smaller the pairing scale) but $T_c^{\max}$ is in the opposite trend. The fact that $Ca_{2-x}Na_xCuO_2Cl_2$ can be synthesized only under high pressure renders the difficulty in preparation of high-quality samples,[48,49] which may account for the "antitrend" low T_c. Interestingly, when it comes to compare $Ca_{2-x}Na_xCuO_2Cl_2$ with $Sr_2CuO_2F_{2+\delta}$ ($T_c^{\max}=46$ K, also synthesized under high pressure and presumably having a similar degree of structural impurity and compositional inhomogeneity), the anticorrelation between $T_c^{\max}$ and V_{ij} now applies.

The material-dependent effects of V_{ij} should be distinguished from those of the t' and t'' terms, which arguably affects HTSC by altering the van Hove singularity in the band structure.[10] In fact, due to the anticorrelation between V_{ij} and $|t'/t|$ as shown in Fig. 3(c), the pairing scale would *appear to* correlate with $|t'/t|$.

With regard to charge distribution, modulation of μ_i tends to induce charge inhomogeneity. As shown in Fig. 3(a), μ_i depends strongly on the apical environment and is mainly determined by the electrostatic potential[50] and strongly enhanced vacuum fluctuations depicted in Fig. 5. In multilayer systems, only the two outer CuO_2 planes have apical atoms; therefore, μ_i in the outer and inner CuO_2 layers can be considerably different. This explains strong *interlayer* charge imbalance in the multilayer systems such as $HgBa_2Ca_{n-1}Cu_nO_{2n+2+\delta}$ with $n \geq 3$ (Ref. 51). As for the strong interlayer charge imbalance observed in atomically perfect $La_{1.85}Sr_{0.15}CuO_4/La_2CuO_4$ films[52] where all the layers have apical atoms, a considerable contribution may be made by the change of μ_i due to shifting the relative site energy of the apical P_z state with respect to the in-plane P_s state by substitution of Sr for La in the $La_{1.85}Sr_{0.15}CuO_4$ layers. On the other hand, chemical doping may cause μ_i to fluctuate in space and thus might induce in-plane inhomogeneous distribution of the low-energy quasiparticles.[53] However, the repulsive V_{ij}, which disfavors hole accumulation, effectively counters the fluctuation in μ_i, as they share a similar ε_{P_z} dependence (see Fig. 3). Their net effect is to retain a rather homogeneous in-plane charge distribution.[54]

The present results also shed light on understanding other exotic features of cuprates. For example, recent spectroscopic imaging scanning tunneling microscopy (SI-STM) on $Bi_2Sr_2CaCu_2O_{8+\delta}$ revealed a puzzling coexistence of strong modulation of local pairing gaps (correlated with oxygen dopants, O_δ) and surprisingly weak low-energy charge-density variations.[55] These striking results have been phenomenologically attributed to a strong local modulation of electron pairing strength,[56] J in the *t-J* model,[57] or μ_i with two types of O_δ.[58] The present studies suggest that O_δ perturb ε_{P_z} and thus modulate V_{ij} and μ_i, etc. On the one hand, the variation of V_{ij} affects the local pairing scale. On the hand other, $Bi_2Sr_2CaCu_2O_{8+\delta}$ has only one type of CuO_2 planes (i.e., there are no distinct inner and outer planes); as mentioned above, the competition between μ_i and V_{ij} retains the in-plane homogeneous distribution of the low-energy quasiparticles. This scenario would also account for more recent SI-STM data that reveal a strong correlation between the local superconducting gap size and the Cu-O_{apical} distance.[59]

Furthermore, the strong ε_{P_z} dependence of t', t'', V_{ij}, and μ_i implies that electron-phonon interactions involving the vibration of apical atoms may be strong. In particular, the V_{ij} variation in this way yields an intriguing phonon-mediated interaction between a pair of electrons with another pair. The determination of their actual strengths will be pursued elsewhere.

Finally, our findings support the significance of examining HTSC in multilayer systems,[51,52] as the influence of the apical P_z orbitals will be significantly layer dependent and can be controlled (e.g., via strain and field effects) to tune hole-hopping range, distribution, and super repulsion among the CuO_2 layers.

ACKNOWLEDGMENTS

We thank S. R. White for advice on numerical canonical transformation.[60] Discussions with O. K. Andersen, P. W. Anderson, I. Bozovic, J. C. Davis, T. K. Lee, D. C. Mattis, W. E. Pickett, T. M. Rice, G. A. Sawatzky, R. T. Scalettar, A. M. Tsvelik, and Z. Wang are acknowledged. This work was supported by U.S. DOE under Grant No. DE-AC02-98CH10886 and CMSN.

*wyin@bnl.gov
†weiku@bnl.gov

[1] P. W. Anderson, P. A. Lee, M. Randeria, T. M. Rice, N. Trivedi, and F. C. Zhang, J. Phys.: Condens. Matter **16**, R755 (2004).
[2] E. Dagotto, Rev. Mod. Phys. **66**, 763 (1994).
[3] P. A. Lee, N. Nagaosa, and X.-G. Wen, Rev. Mod. Phys. **78**, 17 (2006).
[4] F. C. Zhang and T. M. Rice, Phys. Rev. B **37**, 3759 (1988).
[5] H. Eskes and G. A. Sawatzky, Phys. Rev. Lett. **61**, 1415 (1988).
[6] A. K. McMahan, R. M. Martin, and S. Satpathy, Phys. Rev. B **38**, 6650 (1988).
[7] M. S. Hybertsen, E. B. Stechel, M. Schluter, and D. R. Jennison, Phys. Rev. B **41**, 11068 (1990).
[8] A. Damascelli, Z.-X. Shen, and Z. Hussain, Rev. Mod. Phys. **75**, 473 (2003).
[9] Y. Ohta, T. Tohyama, and S. Maekawa, Phys. Rev. B **43**, 2968 (1991).
[10] L. F. Feiner, J. H. Jefferson, and R. Raimondi, Phys. Rev. Lett. **76**, 4939 (1996).
[11] R. Raimondi, J. H. Jefferson, and L. F. Feiner, Phys. Rev. B **53**, 8774 (1996).
[12] E. Pavarini, I. Dasgupta, T. Saha-Dasgupta, O. Jepsen, and O. K. Andersen, Phys. Rev. Lett. **87**, 047003 (2001).
[13] K. Tanaka, T. Yoshida, A. Fujimori, D. H. Lu, Z.-X. Shen, X.-J. Zhou, H. Eisaki, Z. Hussain, S. Uchida, Y. Aiura, K. Ono, T. Sugaya, T. Mizuno, and I. Terasaki, Phys. Rev. B **70**, 092503 (2004).
[14] W.-G. Yin, C. D. Gong, and P. W. Leung, Phys. Rev. Lett. **81**, 2534 (1998).
[15] T. Valla, A. V. Fedorov, J. Lee, J. C. Davis, and G. D. Gu, Science **314**, 1914 (2006).
[16] S. R. White and D. J. Scalapino, Phys. Rev. B **60**, R753 (1999).
[17] Th. Maier, M. Jarrell, Th. Pruschke, and J. Keller, Phys. Rev. Lett. **85**, 1524 (2000).
[18] C. T. Shih, T. K. Lee, R. Eder, C.-Y. Mou, and Y. C. Chen, Phys. Rev. Lett. **92**, 227002 (2004).
[19] J. M. Tranquada, S. M. Heald, A. R. Moodenbaugh, and M. Suenaga, Phys. Rev. B **35**, 7187 (1987).
[20] A. Fujimori, E. Takayama-Muromachi, Y. Uchida, and B. Okai, Phys. Rev. B **35**, 8814 (1987).
[21] C. T. Chen, F. Sette, Y. Ma, M. S. Hybertsen, E. B. Stechel, W. M. C. Foulkes, M. Schluter, S.-W. Cheong, A. S. Cooper, L. W. Rupp, Jr., B. Batlogg, Y. L. Soo, Z. H. Ming, A. Krol, and Y. H. Kao, Phys. Rev. Lett. **66**, 104 (1991).
[22] W.-G. Yin, D. Volja, and W. Ku, Phys. Rev. Lett. **96**, 116405 (2006).
[23] W. Ku, H. Rosner, W. E. Pickett, and R. T. Scalettar, Phys. Rev. Lett. **89**, 167204 (2002).
[24] Strong material dependence of ε_{P_z} was also shown to exist in the ionic model (Ref. 9).
[25] V. I. Anisimov, M. A. Korotin, A. S. Mylnikova, A. V. Kozhevnikov, D. M. Korotin, and J. Lorenzana, Phys. Rev. B **70**, 172501 (2004).
[26] K. Schwarz, P. Blaha, and G. K. H. Madsen, Comput. Phys. Commun. **147**, 71 (2002).
[27] C. T. Chen, L. H. Tjeng, J. Kwo, H. L. Kao, P. Rudolf, F. Sette, and R. M. Fleming, Phys. Rev. Lett. **68**, 2543 (1992).
[28] W. E. Pickett, Rev. Mod. Phys. **61**, 433 (1989).
[29] T. Kostyrko, Phys. Rev. B **40**, 4596 (1989).
[30] J. Hubbard, Proc. R. Soc. London, Ser. A **285**, 542 (1965).
[31] J. H. Jefferson, H. Eskes, and L. F. Feiner, Phys. Rev. B **45**, 7959 (1992).
[32] D. C. Mattis, Phys. Rev. Lett. **74**, 3676 (1995).
[33] R. Raimondi, J. H. Jefferson, and L. F. Feiner, Phys. Rev. B **53**, 8774 (1996).
[34] C. Kim, P. J. White, Z. X. Shen, T. Tohyama, Y. Shibata, S. Maekawa, B. O. Wells, Y. J. Kim, R. J. Birgeneau, and M. A. Kastner, Phys. Rev. Lett. **80**, 4245 (1998).
[35] B. O. Wells, Z. X. Shen, A. Matsuura, D. M. King, M. A. Kastner, M. Greven, and R. J. Birgeneau, Phys. Rev. Lett. **74**, 964 (1995).
[36] F. Ronning, C. Kim, D. L. Feng, D. S. Marshall, A. G. Loeser, L. L. Miller, J. N. Eckstein, I. Bozovic, and Z. X. Shen, Science **282**, 2067 (1998).
[37] S. Schmitt-Rink, C. M. Varma, and A. E. Ruckenstein, Phys. Rev. Lett. **60**, 2793 (1988).
[38] P. W. Leung and R. J. Gooding, Phys. Rev. B **52**, R15711 (1995).
[39] V. I. Belinicher, A. L. Chernyshev, and V. A. Shubin, Phys. Rev. B **54**, 14914 (1996).
[40] T. Xiang and J. M. Wheatley, Phys. Rev. B **54**, R12653 (1996).
[41] P. W. Leung, B. O. Wells, and R. J. Gooding, Phys. Rev. B **56**, 6320 (1997).
[42] P. W. Anderson, Science **316**, 1705 (2007).
[43] E. Dagotto, A. Nazarenko, and A. Moreo, Phys. Rev. Lett. **74**, 310 (1995).
[44] The long-range Coulomb interaction is also appreciable in determining the charge patterns, see E. Arrigoni, A. P. Harju, W. Hanke, B. Brendel, and S. A. Kivelson, Phys. Rev. B **65**, 134503 (2002).
[45] C. C. Tsuei and J. R. Kirtley, Rev. Mod. Phys. **72**, 969 (2000).
[46] V. J. Emery and S. A. Kivelson, Nature (London) **374**, 434 (1995).
[47] S. A. Kivelson, Physica B **318**, 61 (2002).
[48] Y. Kohsaka, M. Azuma, I. Yamada, T. Sasagawa, T. Hanaguri, M. Takano, and H. Takagi, J. Am. Chem. Soc. **124**, 12275 (2002).
[49] Z. Hiroi, N. Kobayashi, and M. Takano, Physica C **266**, 191 (1996).
[50] M. Di Stasio, K. A. Müller, and L. Pietronero, Phys. Rev. Lett. **64**, 2827 (1990).
[51] H. Mukuda, M. Abe, Y. Araki, Y. Kitaoka, K. Tokiwa, T. Wa-

tanabe, A. Iyo, H. Kito, and Y. Tanaka, Phys. Rev. Lett. **96**, 087001 (2006).
[52] I. Bozovic, G. Logvenov, M. A. J. Verhoeven, P. Caputo, E. Goldobin, and T. H. Geballe, Nature (London) **422**, 873 (2003).
[53] Z. Wang, J. R. Engelbrecht, S. Wang, H. Ding, and S. H. Pan, Phys. Rev. B **65**, 064509 (2002).
[54] P. Abbamonte, L. Venema, A. Rusydi, I. Bozovic, and G. A. Sawatzky, Science **297**, 581 (2002).
[55] K. McElroy, J. Lee, J. A. Slezak, D.-H. Lee, H. Eisaki, S. Uchida, and J. C. Davis, Science **309**, 1048 (2005).
[56] T. S. Nunner, B. M. Andersen, A. Melikyan, and P. J. Hirschfeld, Phys. Rev. Lett. **95**, 177003 (2005).
[57] J.-X. Zhu, arXiv:cond-mat/0508646 (unpublished).
[58] S. Zhou, H. Ding, and Z. Wang, Phys. Rev. Lett. **98**, 076401 (2007).
[59] J. A. Slezak, J. Lee, M. Wang, K. McElroy, and K. Fujita, B. Mersen, P. J. Hirschfeld, H. Eisaki, S. Uchida, and J. C. Davis, Proc. Natl. Acad. Sci. U.S.A. **105**, 3203 (2008).
[60] S. R. White, J. Chem. Phys. **117**, 7472 (2002).